JOURNAL OF OPTOELECTRONICS AND ADVANCED MATERIALS, Vol. 11, No. 1, January 2009, p. 56 - 61

Theoretical calculation of enhancement factor of third-order nonlinear susceptibility in gold nanowire and nanotube

JIAN ZHU[a,*], XIA HUANG[a], JIAN-JUN LI[b], JUN-WU ZHAO[b]
[a] *School of Science, Xi'an Jiaotong University, Xi'an 710049, China*
[b] *School of Life Science and Technology, Xi'an Jiaotong University, Xi'an 710049, China*

The third-order nonlinear optical properties in gold nanowire and nanotube were theoretical studied by using quasi-static approximation. The enhancement factor patterns of the third-order nonlinear optical susceptibility in both gold nanowire and nanotube are anisotropic. For gold nanowire and the symmetric mode of nanotube, the "hot spots" of positive or negative nonlinear enhancement factors occur close to the poles of the wire or tube along the incident polarization direction. Whereas for antisymmetric mode of nanotube, the "hot spots" of positive or negative nonlinear enhancement factors occur within the gold tube and locate close to the poles of the tube along or perpendicular to the incident polarization direction. These calculation results show that the pattern of the third-order nonlinear enhancement factor is controlled by the fluctuation in surface electrons and the distribution of local electric field. These tunable third-order nonlinear optical characteristic will help us to select the best morphology of gold nanotube for the fabrication of smart optical nano-sensors.

(Received August 7, 2008; accepted January 21, 2009)

Keywords: Gold, Nanotube, Nanowire, Third-order nonlinear susceptibility, Pattern

1. Introduction

Nanometer sized composite systems of noble metal nanoparticles embedded in dielectric surroundings often exhibit large third-order optical nonlinearities response because of the enhancement of the local field near and inside the metal particles [1-11]. In 1985, Ricard *et al*. [1] have already measured the third-order nonlinear susceptibility of gold colloidal solutions. Zhou *et al*. [2] found that the maximum value of $\chi^{(3)}$ of Ag:Bi_2O_3 thin films occurs at an annealing temperature of 600°C. Olivares *et al*. [3] reported the large enhancement of the third-order optical susceptibility in Cu-silica composites produced by low-energy high-current ion implantation. Lippitz *et al*. [4] reported the first observation of third-harmonic signals from individual gold colloids down to 40 nm diameter. The third-harmonic intensity varies as the square of the colloid surface area. In the paper of Fei *et al*. [5], the third-order nonlinear optical susceptibility $\chi^{(3)}$ of nanoscale silver particles dispersed in silicon oil and surface-modified nanoscale silver particles dispersed in silicon oil were measured by a third harmonic generation method. It is suggested that local field effect and the inter-band transition of electrons from the surface state to the unoccupied state near the Fermi level played important roles in the enhancement of $\chi^{(3)}$ for the nanoscale silver particles.

These nonlinear responses have attracted attention because they can be tuned by the particle's size, shape, structure and surroundings [12-15]. In the letter of Ma *et al*. [12], the third-order nonlinear optical response of the gold nanocrystals embedded in $BaTiO_3$ and ZrO_2 matrices was investigated through the off-resonance femto-second optical Kerr effect. Compared with pristine films, the nonlinearity of composite films shows an enhancement, which is dependent on the size of gold particle and the refractive index of the matrices. Drachev *et al*. [13] have calculated size dependence of the $\chi^{(3)}$ for Ag nanoparticles. Pincon *et al*. [14] reported a study about the third-order nonlinear optical properties of nanocomposite thin films composed of gold particles embedded in a silica host matrix. They especially studied the effect of the metal concentration and the influence of thermal treatment on the real and imaginary components of the third-order nonlinear susceptibility. They finally point out that the material nonlinear properties are greatly sensitive to the incident wavelength through the local field enhancement phenomenon. In the paper of Gao *et al*. [15], temperature-dependent nonlinear optical properties including the real part, imaginary part and the magnitude of effective nonlinear optical susceptibility in metal-dielectric composites have been studied by means of the decoupling approximation and spectral representation. Hamanaka *et al*. [16] and Shen *et al*. [17] also investigated the third-order nonlinear optical susceptibilities $\chi^{(3)}$ of Au-Silica core-shell nanoparticles and periodic triangular Au nanoparticle arrays, respectively.

Recently, the noble metal nanowire and nanotube have received much attention as low dimensional structures, which due to their possible future chemical and physical applications [18-21]. Sun *et al*. [18] have fabricated nanorattles consisting of Au/Ag alloy cores and Au/Ag alloy shells by starting with Au/Ag alloy colloids as an

initial template. They have also prepared multiple-walled nanoshells/nanotubes with a variety of shapes, compositions, and structures by controlling the morphology of the template and the precursor salt used in each step of the replacement reaction. Helical gold nanotubes have been synthesized by Oshima *et al*. at 150 K [19], the gold single wall nanotube is composed of five atomic rows that coil about the tube axis. Our previous studies show that the second-harmonic generation (SHG) enhancement factor in gold nanotubes is tunable by the polarization direction, wall thickness and dielectric environment [22]. It is well known that there is a significant influence of spatial distance and direction on the optical response. So the distributions of the outside electric filed of particles should be investigated with spatial distance and direction. Hao *et al*. [23] and Schelm *et al*. [24] have investigated the distribution of the outside and internal electric field of the nanoshells. We also have reported on the distribution of outside electric field around the nanowire recently [25]. Then, how about the third-order nonlinear optical properties of these noble metal nanowires and nanotubes? In this letter, we report on the third-order nonlinear enhancement factor patterns in gold nanowires and nanotubes. Calculation results based on quasi-static theory show these gold nanowires and single wall nanotubes being exhibit large third-order optical nonlinearities enhancement because of the local field near and in the gold nanostructure. Furthermore, both real and imaginary parts of these nonlinear enhancement factors have different anisotropic distribution patterns.

2. The model

A schematic illustration of our model, including a nanowire and a nanotube geometry is given in Figure 1. It consists of an infinite gold cylinder of radius r_1 (see Figure 1(a)) and an infinite gold tube of core radius r_1 and wall thickness r_2-r_1 (see Fig. 1(b)), which is illuminated by an x-axis directional polarized incident field with its wave vector $\boldsymbol{k}$ along the y-axis. The gold wire and gold wall in tube have a dielectric function ε_1, and the embedding medium has a dielectric constant ε_2. It is important to note that, ε_1 can have real and imaginary frequency-dependent components [26].

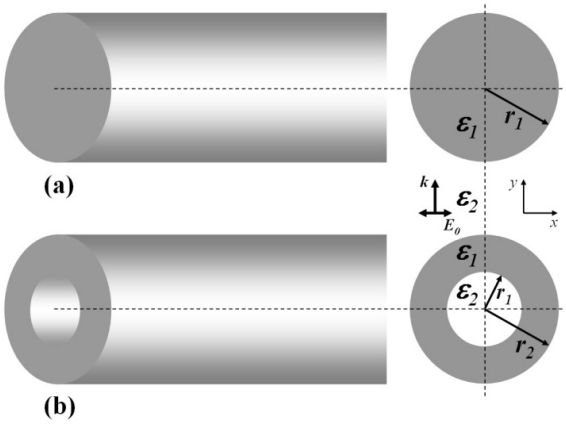

Fig. 1. Schematic of two structures (a) Nanowire, (b) Nanotube.

A great deal of theoretical and numerical methods (such as Finite-Difference Time-Domain (FDTD) [27], extended Mie scattering theory [28], Discrete Dipole Approximation (DDA) [29]) have been carried out to determine the electric field behavior in the case of visible light interacting with nanostructures. Here, we use the quasi-static theory to study the optical properties of gold nanowire and nanotube. Quasi-static theory assumes that the radius of the gold particle is far small relative to the wavelength of light. Therefore the gold particle is subjected to an almost uniform field, and then oscillates like a simple dipole with polarization proportional to the incident field, considerably simplifying the calculations [30]. In our calculation, the radius (22.5 nm) of wire and tube is much smaller than the wavelength (400~1000 nm). So, we consider that the model used in this paper is suitable for the quasi-static calculation. The electric field in each region of the gold wire could be derived from *Laplace*'s equation. When the incident electric field is $\boldsymbol{E_0}$, the solution for the local electric field in the gold wire ($\boldsymbol{E_1}$) and surrounding dielectric regions ($\boldsymbol{E_2}$) are given by [31]

$$\vec{E}_1 = \frac{2\varepsilon_1}{\varepsilon_1+\varepsilon_2} E_0 \vec{e}_x \quad , \tag{1}$$

$$\vec{E}_2 = E_0\vec{e}_x + \left(\frac{\varepsilon_1-\varepsilon_2}{\varepsilon_1+\varepsilon_2}\cdot\frac{r_1^2}{r^2}\right)E_0(\cos 2\phi\vec{e}_x + \sin 2\phi\vec{e}_y) \tag{2}$$

similarly, for a single gold tube, the solution for the local electric field in the dielectric core ($\boldsymbol{E_1}$), gold wall ($\boldsymbol{E_2}$) and surrounding dielectric regions ($\boldsymbol{E_3}$) are given by [31]

$$\vec{E}_1 = \frac{4\varepsilon_1\varepsilon_2 r_2^2}{(\varepsilon_1+\varepsilon_2)^2 r_2^2 - (\varepsilon_1-\varepsilon_2)^2 r_1^2} E_0\vec{e}_x \tag{3}$$

$$\vec{E}_2 = \frac{2(\varepsilon_2^2+\varepsilon_1\varepsilon_2)r_2^2}{(\varepsilon_1+\varepsilon_2)^2 r_2^2 - (\varepsilon_1-\varepsilon_2)^2 r_1^2} E_0\vec{e}_x + \\ + \frac{2(\varepsilon_2^2-\varepsilon_1\varepsilon_2)r_1^2 r_2^2}{(\varepsilon_1+\varepsilon_2)^2 r_2^2 r^2 - (\varepsilon_1-\varepsilon_2)^2 r_1^2 r^2} E_0(\cos 2\phi\vec{e}_x + \sin 2\phi\vec{e}_y) \quad , \tag{4}$$

$$\vec{E}_3 = E_0\vec{e}_x + \frac{(\varepsilon_2^2-\varepsilon_1^2)(r_1^2 r_2^2 - r_2^4)}{(\varepsilon_1+\varepsilon_2)^2 r_2^2 r^2 - (\varepsilon_1-\varepsilon_2)^2 r_1^2 r^2} E_0(\cos 2\phi\vec{e}_x + \sin 2\phi\vec{e}_y) \quad , \tag{5}$$

where ϕ is the azimuthal angle that the incident field makes with the position vector $\boldsymbol{r}$.

The effective third-order nonlinear susceptibility $\chi^{(3)}$ is a nonlinear optical parameter standing for the effective value which is defined over the volume of the composite material illuminated by the laser beam. Many studies on composites with very low metal volume fraction have

simplified the expression of $\chi^{(3)}$ by using a mean field approximation in which fluctuations of the local electric field inside each component of the medium are neglected [32]. Under such an assumption, the effective third-order nonlinear susceptibility $\chi^{(3)}$ can be written as [32-34]

$$\chi^{(3)}(\omega) = p\left|f(\omega)\right|^2 f^2(\omega)\chi_m^{(3)}(\omega), \quad (6)$$

where $\chi_m^{(3)}(532nm) = \chi_{mr} + i\chi_{mi} = (-1+5i)\times 10^{-8} esu$ is the intrinsic third-order nonlinear susceptibility of gold particles [14,35], p denotes the gold concentration. The quantity appearing in the above equation, f, called local-field enhancement factor [14], is the ratio between the electric field in the gold particle and the applied field E_{Local}/E_0. It is obvious that the third-order nonlinearity of the gold nanostructure can be enhanced by an amount equal to the fourth power of the local field factor, close to the SPR frequency. Indeed, the local electric field changes its intensity and direction from the point position, i.e. there is a significant influence of r and ϕ on the local field factor distribution around metal nanoparticles. In order to find the distribution fashion of the enhancement factor of the third-order nonlinear optical response $f^{(3)}$, we take the *"r"* and *"ϕ"* dependent local field factor, see Eqs. (1)-(5), into the calculation of third-order nonlinear susceptibility. It is important to note that the local-field factor is a complex number, because the dielectric constant of gold nanoparticles is a complex number. Therefore, we can obtain real and imaginary components of the third-order nonlinear susceptibility

$$\mathrm{Re}(\chi^{(3)}) = p\left|f\right|^2[(f_r^2 - f_i^2)\chi_{mr} - 2f_r f_i \chi_{mi}], \quad (7)$$

$$\mathrm{Im}(\chi^{(3)}) = p\left|f\right|^2[(f_r^2 - f_i^2)\chi_{mi} + 2f_r f_i \chi_{mr}] \quad (8)$$

where f_r and f_i are the real and imaginary components of the local-field factor. It is obvious that both the real and imaginary components of the third-order nonlinear susceptibility are enhanced by local-field enhancement factor. The real and imaginary components of the enhancement factor of third-order nonlinear optical response can be written as

$$\mathrm{Re}(f^{(3)}) = \left|f\right|^2[(f_r^2 - f_i^2) - 2f_r f_i], \quad (9)$$

$$\mathrm{Im}(f^{(3)}) = \left|f\right|^2[(f_r^2 - f_i^2) + 2f_r f_i]. \quad (10)$$

3. Results and discussion

The calculated third-order nonlinear enhancement factors of the nanowire are illustrated in Figure 2. In this calculation, ε_2=1.5 and r_1=22.5nm. It is obvious that the enhancement factors are very sensitive to the incident wavelength through the local field enhancement phenomenon [14]. In the visible range (400-760nm), each spectrum presents a positive peak and a negative peak. The negative peak always takes place around the SPR wavelength, and getting very weak far from SPR wavelength. When we take the value of $\phi=0$, both the negative and positive peaks of the real part are lower than that of the imaginary part respectively. However when $\phi=\pi/2$, both the negative and positive peaks of real part are higher than that of imaginary part respectively. Figure 2 also reveals that greater nonlinear response takes place in the x-axis direction (the polarized direction of the incident light), i.e. $\phi=0$. The negative peak of Re($f^{(3)}$) occurs at 557nm, whereas the positive peak of Im($f^{(3)}$) occurs at 568nm. Pincon *et al*. [14] have reported that "it is possible to get high negative Im$\chi^{(3)}$ value together with a much weaker Re$\chi^{(3)}$ value at some wavelengths close to the SPR". This phenomenon also takes place in our calculation when $\phi=\pi/2$.

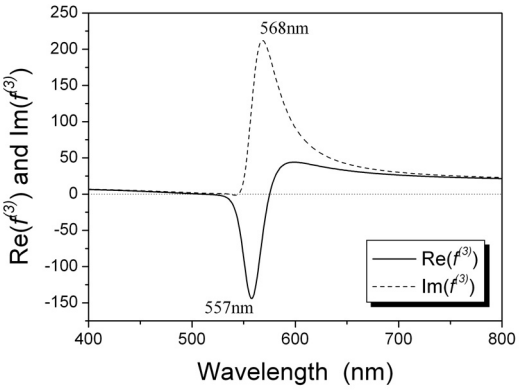

(a)

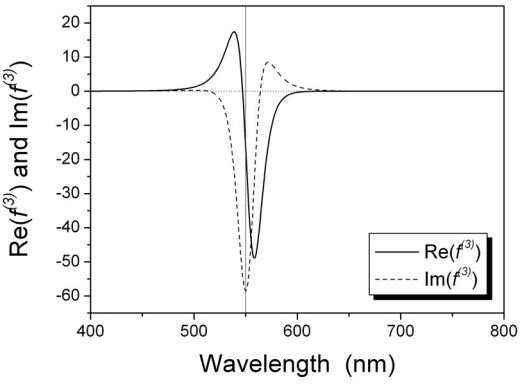

(b)

Fig. 2. The calculated real and imaginary parts of $f^{(3)}$ for a gold nanowire with $r=r_1$ and (a) $\phi=0$; (b) $\phi=\pi/2$.

The distributions of the real and imaginary parts of

third-order nonlinear enhancement factor in the *x-y* plane of gold nanowire are shown in Figure 3(a-b). In this calculation, $\lambda_{resonance}$=552nm ($\lambda_{resonance}$ is the wavelength of the incident light, which is close to the SPR wavelength and coupling to the extremum of the nonlinear enhancement factor). The real part of $f^{(3)}$ around the gold wire are different from direction, as shown in Figure 3(a). In *x* axis direction, Re($f^{(3)}$) has the maximum negative value near to the wire and gets weaker obviously with increasing the distance from gold wire. The distribution fashion of imaginary part of $f^{(3)}$ is different from that of Re($f^{(3)}$) and the anisotropy increases. Im($f^{(3)}$) has the maximum positive value close to the poles of the wire along the incident polarization direction, i.e. *x*-axis direction, whereas the maximum negative value occurs inside the gold wire, as shown in Figure 3(b).

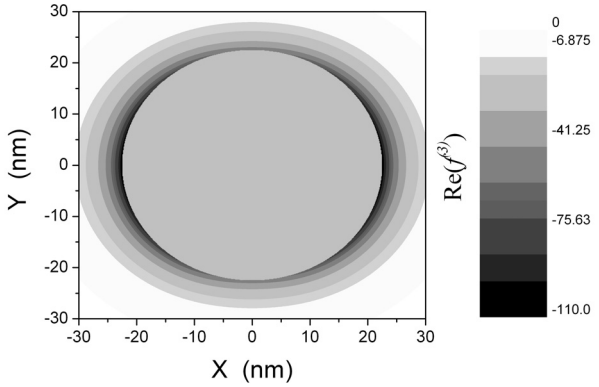

(a)

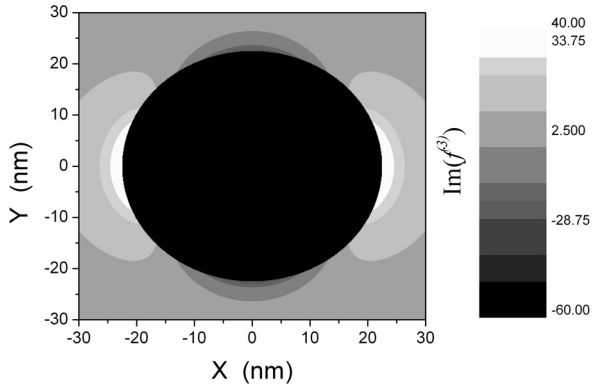

(b)

Fig. 3. The calculated patterns of (a) the real and (b) imaginary parts of $f^{(3)}$ in the x-y plane for a gold nanowire with polarized illumination at 552nm.

The major feature of the nanotube is having two interfaces between gold and dielectric medium, which is different from gold nanowire. Therefore, the *x-y* plane has been divided into three parts by the interfaces. Because of having two dielectric-metallic interfaces, there are two local field factor peaks resulted from the hybridization between the two free plasmon modes, i.e., the wire plasmon which corresponding to outer surface and the well plasmon which corresponding to inner surface. The longer wavelength peak corresponds to the lower energy symmetric or "bonding" plasmon and the shorter wavelength peak corresponds to the higher energy antisymmetric or "antibonding" plasmon [20]. The distributions of real and imaginary parts of the third-order nonlinear enhancement factor in the *x-y* plane of gold nanotube are shown in Figure 4. For symmetric mode, $\lambda_{resonance}$=726nm, both the real and imaginary parts of the third-order nonlinear response are enhanced greatly. The distributions of nonlinear enhancement factor in the surrounding medium are similar to that of gold nanowire, whereas the anisotropy decreases. The maximum negative value occurs inside the dielectric core, as shown in Figure 4(a-b). For symmetric mode, $\lambda_{resonance}$=538nm, both the real and imaginary parts of the third-order nonlinear response are enhanced slightly. The maximum positive value occurs inside the dielectric core, whereas the maximum negative value occurs inside the gold wall. There are four high negative value areas, which densely locates close to the poles of the gold wall and along or perpendicular to the direction of incident light. For Re($f^{(3)}$), the high negative areas appears close to the inner surface of the gold wall. Whereas for Im($f^{(3)}$), the high negative areas appears close to the outer surface of the gold wall, see Figure 4(c-d).

These calculation results show that the pattern of the third-order nonlinear enhancement factor is controlled by the distribution of local electric field. For symmetric mode, the local fields are repelled out of the gold wall and concentrate in the region around the gold tube. Therefore, the great changing of the third-order nonlinear enhancement factor always takes place out of the gold tube, which is similar to that of gold nanowires. For symmetric mode, the local electric fields concentrate within the gold wall. Therefore, the great changing of the third-order nonlinear enhancement factor always takes place inside the gold wall. The generation of many nonlinear optical properties is due to fluctuation of the density or orientation of molecules or nanoparticles, which instantaneously breaks the centrosymmetry of isotropic media and provides nonlinear conditions. In gold nanoparticles, the collective oscillations of free electrons in metal surface create a fluctuation in surface electrons. So we think that the third-order nonlinear enhancement is due to the fluctuation of the density of oscillatory electrons in gold nanowire and nanotube. Therefore, the “hot” areas of third-order nonlinear enhancement factor always take place at the gold-dielectric interface.

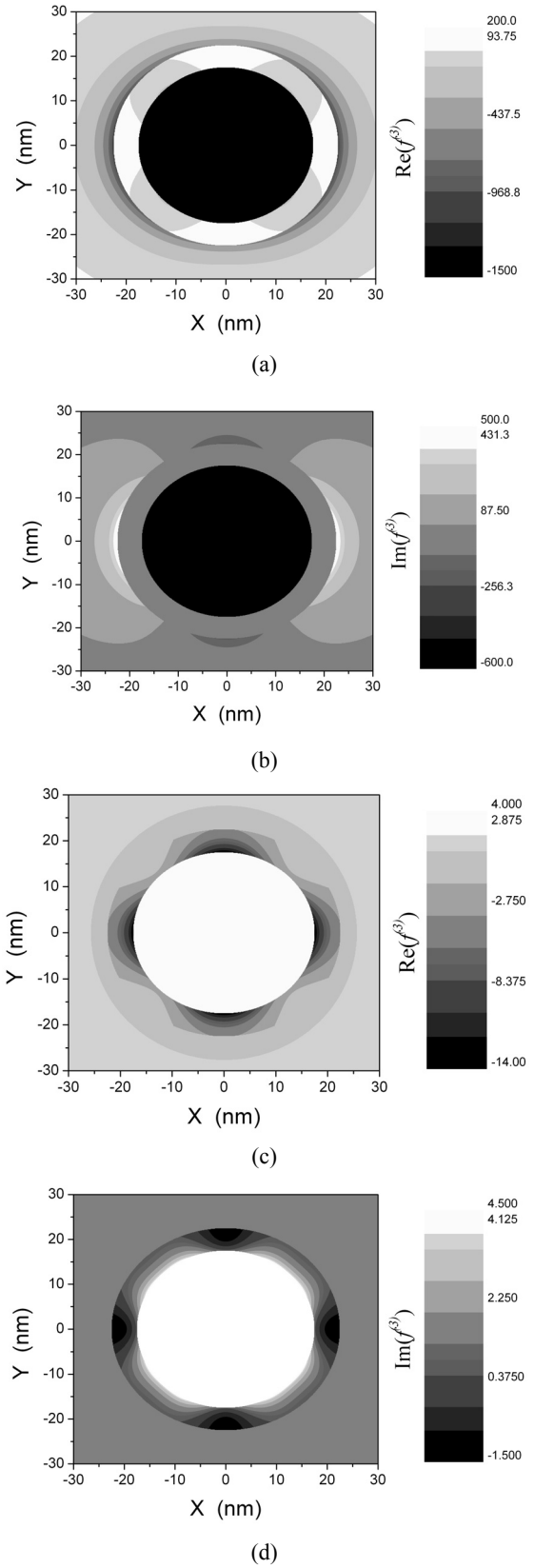

Fig. 4. The calculated patterns of (a) the real and (b) imaginary parts of $\chi^{(3)}$ in the x-y plane for an gold nanotube with polarized illumination at λ=726nm (symmetric mode); (c) the real and (d) imaginary parts of $\chi^{(3)}$ in the x-y plane for an gold nanotube with polarized illumination at λ=538nm (antisymmetric mode).

Knowing how to tune the nonlinear optical properties of metallic nanotubes is of great importance in application fields of nonlinear optical device at the nanoscale. For example, the gold nanotubes can act as conduits for molecule and ion transport [36-37]. Different medium may have different dielectric constant and results in the changing of the external susceptibility patterns of gold nanotube. So the tunable optical signals may help us to distinguish the transported matter or monitoring the flowing behaviour. Furthermore, we can also realize real time detection chemical reaction in the gold tube by detecting the third-order optical susceptibility. Gold nanotubules arrays are also used as new materials for sensing and biosensing [38-39]. The third-order nonlinear optical characters are sensitive to the diameter and wall thickness of gold nanotube, so our calculations will be an effective guide for selection of the best morphology of gold nanotube for the assembling of smart optical sensors and biosensors.

4. Conclusion

Enhancement factor patterns of the third-order nonlinear optical susceptibility in gold nanowire and nanotube were calculated based on the quasi-static theory. The distributions of Re($f^{(3)}$) and Im($f^{(3)}$) around the nanowire and nanotube are different from direction. In the external space of gold wire and tube, the "hot spots" are close to the poles of the wire and tube along the incident polarization direction. However in the internal space of gold tube, the "hot spots" locate close to the poles of the tube along or perpendicular to the incident polarization direction. These tunable characteristic of third-order nonlinear optical susceptibility around gold nanotube will be an effective guide for the design of optoelectronic devices with gold nanostructures.

Reference

[1] D. Ricard, P. Roussignol, C. Flytzanis, Opt. Lett. **10**, 511, (1985).
[2] P. Zhou, G.J. You, J. Li, S.Y. Wang, S.X. Qian, L.Y. Chen, Opt. express **13**, 1508 (2005).
[3] J. Olivares, J. R. Isidro, R. del Coso, R. de Nalda, J. Solis, C. N. Afonso, A. L. Stepanov, D. Hole, P. D. Townsend, A. Naudon, J. Appl. Phys. **90**, 1064 (2001).
[4] M. Lippitz, M.A. van Dijk, Michel Orrit, Nano Lett. **5**, 799 (2005).
[5] G.T. Fei, S.H. Ma, Z.F. Ying, L.D. Zhang, Mater. Res. Bull. **34**, 217 (1999).
[6] H. B. Liao, R. F. Xiao, J. S. Fu, P. Yu, G. K. L. Wong, P. Sheng, Appl. Phys. Lett. **70**, 1 (1997).
[7] R. Coso, J. R. Isidro, J. Solis, J. Gonzalo, C. N. Afonso, J. Appl. Phys. **95**, 2755 (2004).

[8] Y. Wang, X.B. Xie, T. Goodson, Nano Lett. **5**, 2379 (2005).
[9] E. M. Kim, S. S. Elovikov, T. V. Murzina, A. A. Nikulin, O. A. Aktsipetrov, M. A. Bader, G. Marowsky, Phys. Rev. Lett. **95**, 227402 (2005).
[10] Q.Q. Wang, S.F. Wang, W.T. Hang, Q.H. Gong, J. Phys. D, **38**, 389 (2005).
[11] V. M. Shalaev, E. Y. Poliakov, V. A. Markel, Phys. Rev. B, **53**, 2437 (1996).
[12] G. Ma, W. Sun, S.H. Tang, H. Zhang, Z. Shen, S. Qian, Opt. Lett. **27,** 1043 (2002).
[13] V. P. Drachev, A.K. Buin, H.Nakotte, V.M. Shalaev, Nano Lett. **4**, 1535(2004).
[14] N. Pincon, B. Palpant, D. Prot, E. Charron, S. Debrus, The Eur. Phys. J. D **19**, 395 (2002).
[15] L. Gao, Z.Y. Li, Phys. Status Solidi B **218**, 571 (2000).
[16] Y. Hamanaka, K. Fukuta, A. Nakamura, L. M. Liz-Marzan, P. Mulvaney, Appl. Phys. Lett. **84**, 4938 (2004).
[17] H. Shen, B.L. Cheng, G.W. Lu, T. Y. Ning, D. Y. Guan, Y. L. Zhou, Z. H. Chen, Nanotechnology **17**, 4274 (2006).
[18] Y. G. Sun, B. J. Wiley, Z. Y. Li, Y. N. Xia, J. Am. Chem. Soc., **126**, 9399 (2004).
[19] Y. Oshima, A. Onga, K. Takayanagi, Phys. Rev. Lett., **91**, 205503 (2003).
[20] E. Prodan, C. Radlo, N.J. Halas, P. Nordlander, Science **302**, 419 (2003)
[21] Y. Sun, Y. Xia, Adv. Mater., **16**, 264 (2004).
[22] J. Zhu, Nanotechnology, **18**, 225702 (2007).
[23] E. Hao, S. Y. Li, R. C. Bailey, S. l. Zou, G. C. Schatz, J. T. Hupp, J. Phys. Chem. B, **108**, 1224 (2004).
[24] S. Schelm, G.B. Smith, J. Phys. Chem. B, **109**, 1689 (2005).
[25] J. Zhu, Appl. Phys. A, **88**, 673 (2007).
[26] J. A. A. J. Perenboom, P. Wyder, F. Meier, Phys. Rep. **78**, 173 (1981).
[27] M. A. Suarez, T. Grosjean, D. Charraut, D. Courjon, Opt. Commun., **270**, 447 (2007).
[28] K. Imura, T. Nagahara, H. Okamoto, Chem. Phys. Lett. **400**, 500 (2004).
[29] Y. He, G.Q. Shi, J. Phys. Chem. B, **109**, 17503 (2005).
[30] R. D. Averitt, S.L. Westcott, N.L. Halas, J. Opt. Soc. Am. B, **16**, 1824 (1999).
[31] J. Zhu, Mater. Sci. Eng. A, **454-455,** 685 (2007).
[32] S. Debrus, J. Lafait, M. May, N. Pincon, D. Prot, C. Sella, J. Venturini, J. Appl. Phys., **88**, 4469 (2000).
[33] Y. Hamanaka, K. Fukuta, A. Nakamura, L. M. Liz-Marzan, P. Mulvaney, J. Luminesc. **108**, 365 (2004).
[34] K. Puech, W.J. Blau, J Nanopart. Res., **3**, 13 (2001).
[35] D. D. Smith, Y. Yoon, R. W. Boyd, J. K. Campbell, L. A. Baker, R. M. Crooks, M. George, J. Appl. Phys., **86**, 6200 (1999).
[36] S. B. Lee, C.R. Martin, J. Am. Chem. Soc. **124**, 11850 (2002).
[37] S. F. Yu, S.B. Lee, C. R. Martin, Anal. Chem., **75**, 1239 (2003).
[38] A. Curulli, F. Valentini, G. Padeletti, A. Cusma, G. M. Ingo, S. Kaciulis, D. Caschera, G. Palleschi, Sensors and Actuators B, **111-112**, 526 (2005).
[39] M. Wirtz, M. Parker, Y. Kobayashi, C. R. Martin, Chemical Record, **2**, 259 (2002).

*Corresponding author. jianzhusummer@163.com